



## Determination of 20-hydroxyeicosatetraenoic acid in microsomal incubates using high-performance liquid chromatography–mass spectrometry (HPLC–MS)

Christopher A. Bolcato<sup>a</sup>, Reginald F. Frye<sup>a,b</sup>, Michael A. Zemaitis<sup>a</sup>,  
Samuel M. Poloyac<sup>a,\*</sup>

<sup>a</sup>Department of Pharmaceutical Sciences, School of Pharmacy, 808 Salk Hall, University of Pittsburgh, Pittsburgh, PA 15261, USA

<sup>b</sup>Center for Clinical Pharmacology, School of Medicine, University of Pittsburgh, Pittsburgh, PA 15261, USA

Received 4 October 2002; received in revised form 12 June 2003; accepted 23 June 2003

### Abstract

20-HETE is a potent, vasoconstrictive arachidonic acid metabolite with a limited number of published methods for quantitative assessment of microsomal formation rate. The purpose of this study was to evaluate the utility of HPLC–MS (negative ESI) for quantitation of rat microsomal 20-HETE enzyme kinetics. Calibration curves were linear over 0.75–16 ng on-column ( $r^2 > 0.996$ ). The intra- and inter-assay precision and accuracy were <15%. Microsomal 20-HETE revealed saturable (100  $\mu\text{M}$ ) kinetics (brain  $K_m$  and  $V_{max}$ :  $39.9 \pm 6.0 \mu\text{M}$  and  $8.7 \pm 0.6 \text{ pmol/min per mg}$ ; liver  $K_m$  and  $V_{max}$ :  $23.5 \pm 3.2 \mu\text{M}$  and  $775.5 \pm 39.8 \text{ pmol/min per mg}$ ; kidney  $K_m$  and  $V_{max}$ :  $47.6 \pm 8.5 \mu\text{M}$  and  $1933 \pm 151 \text{ pmol/min per mg}$ ). This paper demonstrates HPLC–MS as an efficient method for quantitating 20-HETE enzyme kinetics in microsomes from rat tissues. © 2003 Elsevier B.V. All rights reserved.

**Keywords:** Microsomes; 20-Hydroxyeicosatetraenoic acid; Arachidonic acid; CYP4A

### 1. Introduction

Arachidonic acid (AA) is an endogenous fatty acid that is metabolized by multiple enzymatic pathways to form an array of biologically active eicosanoids. These lipid-derived metabolites have various intracellular signaling functions and are implicated in the pathophysiology of various disease states such as diabetes, cancer, atherosclerosis, hypertension, and subarachnoid hemorrhage [1,2]. Once liberated from

membrane phospholipids by the action of phospholipases, AA is bioactivated through cyclooxygenase, lipoxygenase, and CYP450 pathways [1,3]. Cyclooxygenase mediated metabolism of AA results in formation of prostaglandins and thromboxanes [4]; lipoxygenase mediated metabolism of AA results in formation of leukotrienes, regioisomeric cis/trans conjugated hydroxyeicosatetraenoic acids (HETEs), lipoxins, and hepoxillins; and CYP metabolism of AA produces monooxygenated metabolites including multiple epoxyeicosatrienoic acids (EETs), and several HETEs, such as 20- and 19-HETE (omega and omega-1 hydroxylation, respectively; Fig. 1A) by an NADPH-dependent process [3]. Of these AA bioacti-

\*Corresponding author. Tel.: +1-412-624-4595; fax: +1-412-624-1850.

E-mail address: [poloyac@pitt.edu](mailto:poloyac@pitt.edu) (S.M. Poloyac).

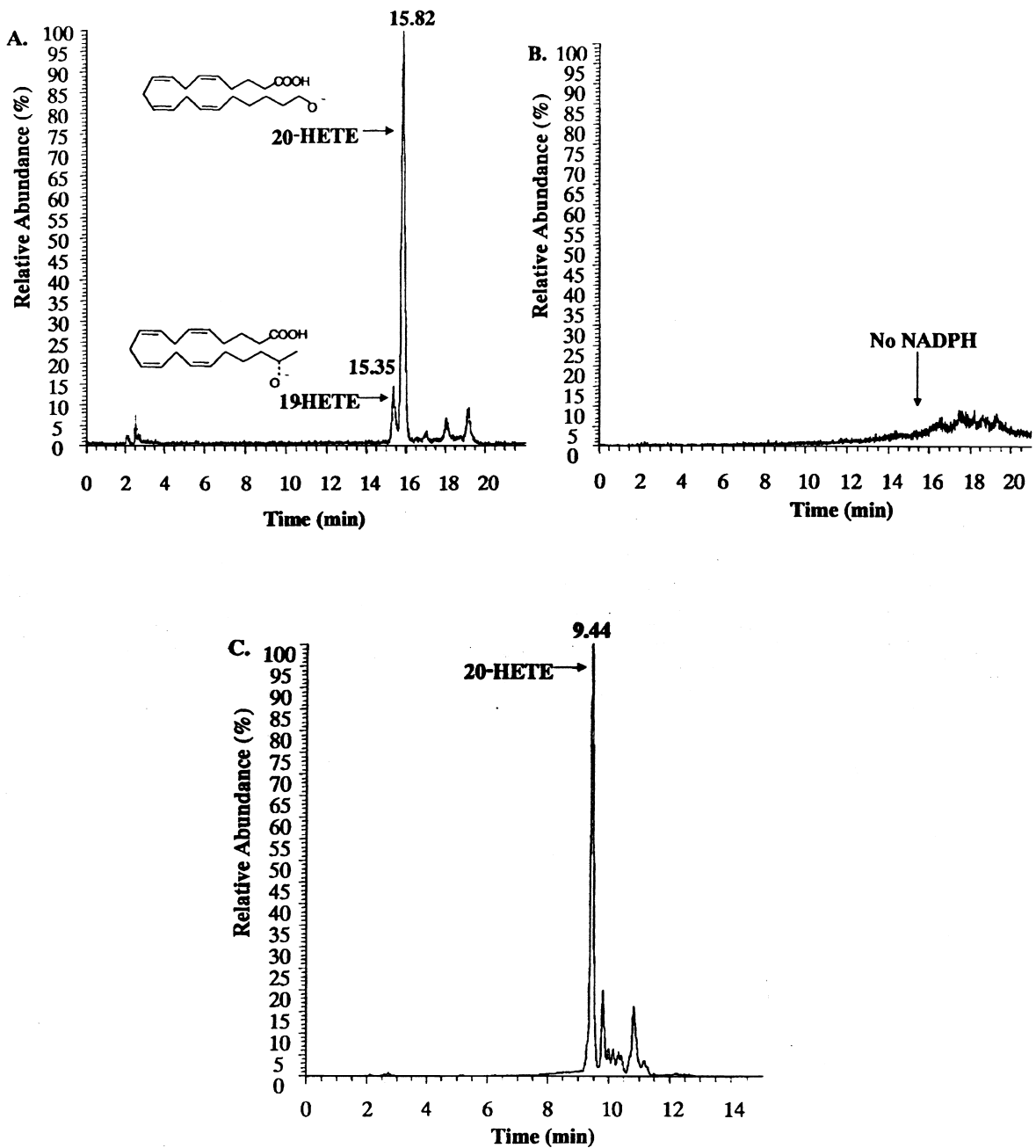


Fig. 1. Representative SIM ( $m/z$  319.5) HPLC-MS chromatograms of rat kidney and brain microsomal incubates: (A) 300  $\mu\text{g}$  kidney microsomal protein incubated with 100  $\mu\text{M}$  AA and 1 mM NADPH for 15 min at 37  $^{\circ}\text{C}$ ; (B) 300  $\mu\text{g}$  kidney microsomal protein incubated with 100  $\mu\text{M}$  AA for 15 min at 37  $^{\circ}\text{C}$  in the absence of NADPH; (C) 1000  $\mu\text{g}$  brain microsomal protein incubated with 100  $\mu\text{M}$  AA and 2 mM NADPH for 60 min at 37  $^{\circ}\text{C}$ .

vation pathways, CYP-mediated formation of 20-HETE produces one of the most potent vasoactive metabolites of AA [5,6]. Although 20-HETE produces cyclooxygenase-dependent effects when applied to large vessels, the predominant site of production is in the microvasculature where it produces potent vasoconstriction [7,8].

Enzymes of the CYP4 family are known to metabolize AA to 20-HETE. Expression of CYP4A isoforms has been documented in liver, kidney, and in the cerebral microvasculature [5,9,10]. Inhibition of 20-HETE formation blocks myogenic responses in renal, cerebral, and skeletal muscle arterioles in vitro and autoregulation of renal and cerebral blood flow in vivo [6,9,11]. Formation of 20-HETE has also been indicated in mediating the effects of various other endogenous agents such as angiotensin II [12], endothelin-1 [13], and nitric oxide [14,15]. A fall in 20-HETE levels produced by nitric oxide inhibition of CYP activity has been implicated as a major mechanism of the cGMP independent effects of nitric oxide [14,15]. Furthermore 20-HETE exerts potent vasoconstriction at concentrations as low as  $10^{-10}$ – $10^{-9}$  M [5,6]. This potency is known to be greater than that of other AA metabolites [16]. Because of its potency and involvement in multiple vasoactive pathways, techniques for assessing 20-HETE concentrations are essential for further evaluating the physiological relevance of 20-HETE. Such techniques would enable the investigation of the regulating biochemical pathways responsible for 20-HETE formation.

A limited number of methods for quantification of 20-HETE have been reported. The most common method employed for assessment of 20-HETE is derivatization and analysis gas chromatography–mass spectrometry (GC–MS) with negative ion chemical ionization [6,17,18]. Another common method used is HPLC with fluorescence or radiochemical detection [19–21]. Although these methods are effective in assessing 20-HETE concentration, they are complicated by lengthy isolation and derivatization steps or need for radiolabeled substrate. HPLC–ESI–MS methods have recently been described for the identification [22] and quantitation [23,24] of AA metabolites. The purpose of this study was to develop an HPLC–MS method that can be used for determination and quantitation of 20-HETE

in microsomal incubates. This method was used to examine the enzyme kinetics of 20-HETE formation in microsomal incubates from rat brain, liver and kidney tissues.

## 2. Experimental

### 2.1. Materials

Authentic 20-HETE and [ $^2\text{H}_8$ ]15(S)-HETE (internal standard) were purchased from Cayman Chemicals (Ann Arbor, MI, USA). Dichloromethane was purchased from Burdick and Jackson (Muskegon, MI, USA). Arachidonic acid, ammonium acetate, and NADPH were purchased from Sigma–Aldrich (St. Louis, MO, USA). All other chemicals were obtained from Fisher Scientific (Pittsburgh, PA, USA) unless otherwise specified.

### 2.2. Microsomal preparation

Rat liver, kidney, and brain microsomal fractions from male Sprague–Dawley rats (Hilltop Labs, Pittsburgh, PA, USA) were obtained by differential centrifugation according to the method of Tindberg et al. with minor modifications [25]. Briefly, animals were anesthetized with ketamine (120 mg/kg) and xylazine (8 mg/kg) intraperitoneally. The brains were perfused via the left ventricle with ice-cold homogenization buffer (50 mM Tris buffer, 150 mM KCl, 0.1 mM dithiothreitol, 1 mM EDTA and 20% glycerol, pH 7.4) containing 0.100 mM PMSF and 0.113 mM BHT. Following perfusion, rats were decapitated and the brain, liver, and kidneys were removed. Tissues were immediately homogenized in fresh buffer and microsomes were obtained via differential centrifugation procedures carried out at 4 °C as previously described [25]. Homogenates were subsequently centrifuged at 18 000 g for 30 min and 125 000 g for 60 min in an L8-70 Ultracentrifuge with a Ti 70.1 rotor (Beckman Coulter, Fullerton, CA, USA). Microsomal pellets were suspended in 20 mM Tris buffer (pH 7.4) containing 250 mM sucrose. Total proteins for microsomes were determined by the method of Lowry et al. [26]. Total P450 content of liver microsomal fractions was determined by P450 spectral analysis [27].

### 2.3. Instrumentation and liquid chromatography–mass spectrometry procedures

#### 2.3.1. HPLC–MS

Metabolites were separated with a ThermoFinnigan Surveyor series HPLC system and detected with an aQa single quadrupole mass spectrometer (ThermoFinnigan, San Jose, CA, USA). The mass spectrometer was operated in negative electrospray ionization mode with a probe voltage of 3.0 kV and temperature of 225 °C. Analysis was carried out using selected ion monitoring (SIM) for specific  $m/z$  319.5 (19- and 20-HETE) and 327.5 ( $[^2\text{H}_8]$ 15(S)-HETE). Data acquisition and analysis were performed with Xcalibur software version 1.2 (ThermoFinnigan, San Jose, CA, USA).

#### 2.3.2. HPLC–MS–MS

For HPLC–MS–MS analysis and product ion identification, metabolites were separated with a TSP SpectraSYSTEM HPLC instrument and detected with an LCQ Duo MS ion trap mass spectrometer (ThermoFinnigan, San Jose, CA, USA). The mass spectrometer was operated in negative electrospray ionization mode with a probe voltage of 4.5 kV and a capillary temperature of 225 °C. The collision energy was set to 36%. Negative ions of  $m/z$  319.5 were monitored and MS–MS spectra of product ions were scanned over the range of  $m/z$  150–325. Data acquisition and analysis were performed with Xcalibur software version 1.2 (ThermoFinnigan, San Jose, CA, USA).

#### 2.3.3. Chromatographic conditions

Separations were carried out at ambient temperature on a reversed-phase, BetaBasic 5  $\mu\text{m}$  C<sub>18</sub> column (150×2 mm) (ThermoHypersil, Bellefont, PA, USA). The two mobile phases consisted of (A) 5 mM ammonium acetate (in deionized water) and (B) methanol. Separation of 20-HETE and  $[^2\text{H}_8]$ 15(S)-HETE in brain and liver microsomal incubates was achieved using a linear gradient from 60 to 95% methanol over 9 min followed by a linear return to initial conditions over 0.2 min, and 6 min of column re-equilibration for a total run time of 15.2 min. The flow rate was 0.2 ml/min. Kidney microsomal incubates were found to produce 19-HETE in

addition to 20-HETE (Fig. 2A). Under the initial chromatographic conditions described, these two metabolites were not completely resolved. Separation of 19-, 20-, and  $[^2\text{H}_8]$ 15(S)-HETE in kidney micro-

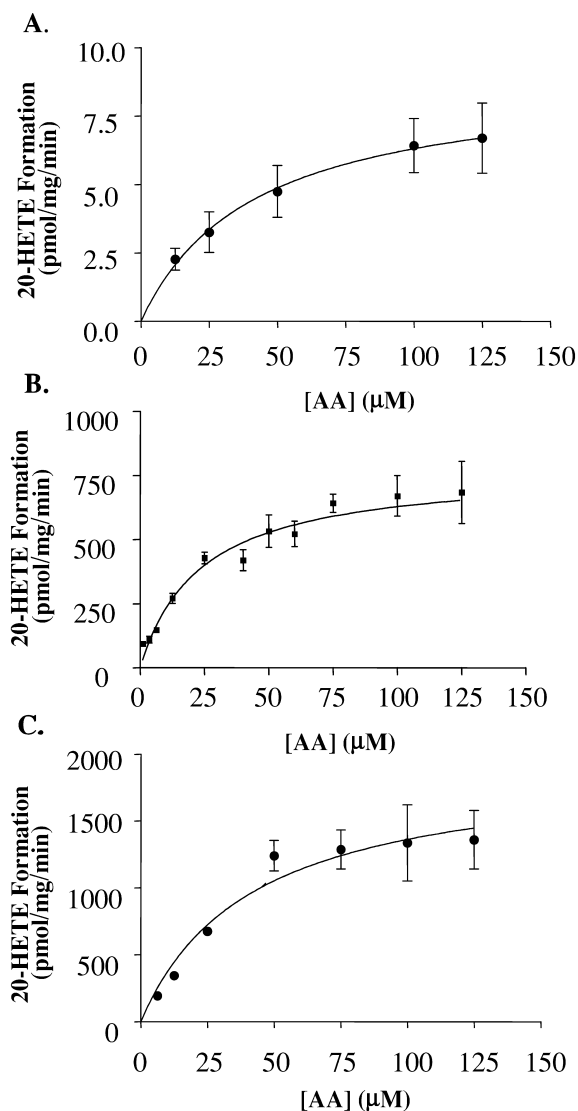


Fig. 2. Effect of arachidonic acid concentration on in vitro 20-HETE formation in rat brain, liver, and kidney microsomal incubates: (A) 1000  $\mu\text{g}$  brain microsomal protein incubated with AA and 2 mM NADPH for 60 min at 37 °C ( $n=4$ ); (B) 300  $\mu\text{g}$  liver microsomal protein incubated with AA and 1 mM NADPH for 15 min at 37 °C ( $n=4$ ); (C) 300  $\mu\text{g}$  kidney microsomal protein incubated with AA and 1 mM NADPH for 15 min at 37 °C ( $n=3$ ).

somal incubates was therefore achieved using a linear gradient of 60–80% methanol over 16 min followed by a linear return to initial conditions over 0.2 min, and 6 min of column re-equilibration for a total run time of 22.2 min. The flow rate was 0.2 ml/min. All injection volumes were 20  $\mu$ l on column.

#### 2.4. Stock solutions, standards, and quality controls (QCs)

Solutions of 20-HETE (5.0 and 0.5 ng/ $\mu$ l) and the internal standard, [ $^2\text{H}_8$ ]15(S)-HETE (5 ng/ $\mu$ l), were prepared by dilution of 100 ng/ $\mu$ l stock solutions (Cayman Chemicals, Ann Arbor, MI, USA) into microsomal incubation buffer (0.12 M potassium phosphate, pH 7.4, containing 5 mM  $\text{MgCl}_2$ ). Dilutions were prepared fresh daily and used for spiking calibration standards and QCs. Preliminary experiments showed that inactivated microsomal protein did not affect the extraction of 20-HETE; therefore, all standards and QCs were prepared in the absence of microsomal protein and NADPH.

#### 2.5. Rat brain, liver, and kidney microsomal incubations

Brain, liver, and kidney microsomal fractions were analyzed for their ability to metabolize AA. Incubations were conducted with 1000 and 300  $\mu$ g of microsomal total protein for brain and liver/kidney, respectively. Incubations were conducted with AA (range 1–150  $\mu$ M) substrate in a total volume of 1 ml of incubation buffer (0.12 M potassium phosphate, pH 7.4, containing 5 mM  $\text{MgCl}_2$ ) as described by Luo et al. [21]. Incubations were begun by the addition of NADPH with final concentrations of

1 and 2 mM NADPH for liver/kidney or brain microsomes, respectively. Solutions were incubated for 15 min at 37  $^\circ\text{C}$  for liver and kidney microsomes or 60 min for brain microsomes. For validation of in vitro 20-HETE formation with respect to time in brain microsomes, 1000  $\mu$ g of microsomal protein was incubated with AA (100  $\mu$ M) at increasing incubation times (20–80 min). For validation of in vitro 20-HETE formation with respect to microsomal protein, samples were incubated for 60 min with AA (100  $\mu$ M) in the presence of varying amounts of microsomal protein from 200 to 1000  $\mu$ g. For HPLC–MS analysis, incubations were stopped by placement of tubes on ice. Due to high enzymatic activity in liver and kidney incubates, 50- $\mu$ l aliquots of the incubates were diluted to a final volume of 1 ml incubation buffer (20-fold dilution) prior to extraction to allow for quantification within the standard curve range. Internal standard (75 ng) was added to all samples followed by double extraction with diethyl ether (3 ml). Samples were evaporated to dryness under nitrogen at 37  $^\circ\text{C}$ , and reconstituted in 200  $\mu$ l of 50:50 methanol:deionized water.

#### 2.6. Calibration and linearity

Calibration curves were constructed using seven standard concentrations of 20-HETE in incubation buffer (1 ml). The amounts of 20-HETE in the spiked standards ranged from 0.75 to 16 ng injected on column (Table 1). Duplicate standard curves were prepared and analyzed over three runs; the lowest standard (0.75 ng) was run in triplicate. For each curve, the peak-area ratios of 20-HETE to the internal standard were calculated and plotted against the amount of 20-HETE injected on column. Cali-

Table 1  
Extraction recoveries for 20-HETE and [ $^2\text{H}_8$ ]15(S)-HETE in various solvents

	Diethyl ether, % recovery	Ethyl acetate, % recovery	Dichloromethane, % recovery	Hexane, % recovery
<i>20-HETE</i>				
Hi QC ( $n=4$ )	89.80 $\pm$ 2.36	86.77 $\pm$ 4.26	86.35 $\pm$ 1.62	13.53 $\pm$ 5.40
Low QC ( $n=4$ )	82.00 $\pm$ 14.58	99.47 $\pm$ 0.39	75.31 $\pm$ 9.56	10.31 $\pm$ 2.23
<i>[<math>^2\text{H}_8</math>]15(S)-HETE</i>				
ISTD level 7.5 ng ( $n=4$ )	95.68 $\pm$ 1.98	88.17 $\pm$ 6.59	98.98 $\pm$ 2.20	25.21 $\pm$ 5.83

bration curves were generated by weighted ( $1/Y$ ) linear regression.

### 2.7. Precision and accuracy

Precision and accuracy were determined by the analysis of 20-HETE QC samples. 20-HETE was spiked into incubation buffer (1 ml) to achieve amounts of 0.8 (low QC), 4.0 (medium QC), and 14 (high QC) ng injected on column. Six replicate QC samples at each amount were analyzed for 2 days, followed by analysis of 12 replicate QC samples at each specified amount on the 3rd day. Means, standard deviations, and relative standard deviations (% RSD) were used to estimate the intra- and inter-assay precision. The calculated mean amount relative to the spiked amount was used to express accuracy (% bias).

### 2.8. Extraction recovery

Extraction recoveries of 20-HETE and [ $^2\text{H}_8$ ]15(*S*)-HETE from incubation buffer were determined in various solvents (diethyl ether, ethyl acetate, dichloromethane, and hexane). Recoveries were determined comparing the responses obtained from extracted samples with those of unextracted reference samples prepared in 50:50 methanol:deionized water. Responses observed for the reference samples were defined as 100%. Extracted samples were found to be stable for at least 48 h at 10 °C in the autosampler. Incubations involving microsomal 20-HETE formation are commonly terminated by addition of formic acid prior to organic extraction [9]. The effects of formic acid concentration and final pH on extraction recoveries of 20-HETE and [ $^2\text{H}_8$ ]15(*S*)-HETE were systematically evaluated over a pH range from 2.0 to 4.0.

### 2.9. Data analysis

Descriptive statistics (mean, SD, C.V.) were calculated using Microsoft Excel. Enzyme kinetic parameter values for maximal velocities ( $V_{\text{max}}$ ) and Michaelis-Menten constants ( $K_m$ ) were determined by weighted ( $1/Y$ ) non-linear regression analysis (Win-Nonlin, Pharsight, Mountainview, CA, USA). Data were fit to one- and two-enzyme Michaelis-Menten

models. Initial parameter estimates used for non-linear regression analysis in a one-enzyme model consisted of the observed  $V_{\text{max}}$  and  $K_m$  values from the substrate saturation experiments. Initial parameter estimates used for non-linear regression analysis in a two-enzyme model consisted of the observed  $V_{\text{max}}$  values and reported  $K_m$  values for CYP4A1, CYP4A2, and CYP4A3 isoforms [28]. Discrimination between one- and two-enzyme Michaelis-Menten kinetic models and the goodness-of-fit were determined by the Akaike information criterion, comparison of the standard errors and coefficients of variation of estimated parameters, and the residual plots.

## 3. Results

### 3.1. Separation of AA metabolites

Fig. 1 illustrates HPLC–MS chromatograms depicting the separation of CYP-dependent AA metabolites derived from rat kidney (Fig. 1A) and brain (Fig. 1C) microsomes incubated with AA (100  $\mu\text{M}$ ). Formed metabolites were verified by MS–MS identification of specific product ions as reported by Bylund et al. [22]. The retention time typically observed for 20-HETE under the HPLC–MS conditions for brain and liver microsomal incubates was 9.4 min (Fig. 1C). The retention times observed for 19-HETE and 20-HETE under the HPLC–MS conditions for kidney microsomal incubates were 15.4 and 15.8 min, respectively (Fig. 1A). Peaks for 19-HETE and 20-HETE were well resolved and no interfering peaks from the sample matrix were observed. In addition, the formation of HETE metabolites in microsomal incubates was demonstrated to be NADPH-dependent (Fig. 1B). The retention times for [ $^2\text{H}_8$ ]15(*S*)-HETE resulting from the liver/brain and kidney gradients were 9.8 and 16.8 min, respectively ( $m/z$  327.5 HPLC–MS data not shown).

### 3.2. Extraction recovery

Multiple solvents were tested and compared for extraction recovery of 20-HETE and [ $^2\text{H}_8$ ]15(*S*)-HETE (Table 1). Mean extraction recoveries of 20-HETE with diethyl ether at the high and low QC

levels were  $89.8 \pm 2.4$  and  $82.0 \pm 14.6\%$ , respectively. Mean extraction recovery of [ $^2\text{H}_8$ ]15(*S*)-HETE (internal standard level, 7.5 ng) was  $95.7 \pm 2.0\%$ . Extraction recovery values for 20-HETE and [ $^2\text{H}_8$ ]15(*S*)-HETE in ethyl acetate and dichloromethane were similar to those obtained with diethyl ether (Table 1). Mean extraction recoveries of 20-HETE with hexane at the high and low QC levels were  $13.5 \pm 5.4$  and  $10.3 \pm 2.2\%$ , respectively. Mean extraction recovery of [ $^2\text{H}_8$ ]15(*S*)-HETE (internal standard level, 7.5 ng) was  $25.2 \pm 5.8\%$ . Termination of incubation reactions by acidification with formic acid prior to extraction is common across the 20-HETE literature [9]. Addition of formic acid resulted in extraction recoveries of  $84.4 \pm 5.3$ ,  $73.1 \pm 7.7$ ,  $66.3 \pm 8.1$ , and  $19.2 \pm 11.8\%$  for 20-HETE versus non-acidified samples at final pH values of 4.01, 3.23, 2.85, and 2.49, respectively. Similarly, extraction of [ $^2\text{H}_8$ ]15(*S*)-HETE in the presence of formic acid resulted in  $73.4 \pm 4.3$ ,  $66.6 \pm 8.7$ ,  $55.2 \pm 6.8$ , and  $16.0 \pm 6.0\%$  versus non-acidified samples at final pH values of 4.01, 3.23, 2.85, and 2.49, respectively. Due to the reduced yield of AA metab-

olites with acidification, microsomal enzymatic reactions were not terminated by the addition of formic acid prior to extraction.

### 3.3. Linearity, precision, and accuracy

Linear calibration curves were obtained for 20-HETE over the range of 0.75–16 ng on column. The mean regression equations ( $\pm$ SD) were as follows:

$$\begin{aligned} \text{20-HETE: } y & \\ &= [0.00018 (\pm 0.00001)]x \pm 0.09672 (\pm 0.01120) \end{aligned}$$

The mean correlation coefficient ( $r^2$ ) was  $>0.996$ . The lower limit of quantification (LOQ) for 20-HETE (0.75 ng on column) was demonstrated to be reproducible (% RSD  $<15\%$ ) with a signal-to-noise ratio of  $\sim 90:1$ . The intra- and inter-run precision and accuracy were within  $\pm 15\%$  for 20-HETE (Table 2). Linearity and reproducibility were demonstrated under all chromatographic conditions described for separation of AA metabolites.

Table 2  
Intra- and inter-day precision and accuracy in incubation buffer

	Amount (ng on column)		% RSD	% Bias
	Added	Observed (mean $\pm$ SD)		
<i>Intra-assay reproducibility</i> <sup>a</sup>				
Quality controls				
20-HETE	0.8	$0.86 \pm 0.03$	14.3	11.2
	4.0	$4.4 \pm 0.1$	3.1	-9.6
	14.0	$12.0 \pm 0.3$	2.6	7.7
<i>Intra-assay reproducibility</i> <sup>b</sup>				
Quality controls				
20-HETE	0.8	$0.85 \pm 0.05$	5.2	-5.8
	4.0	$4.0 \pm 0.5$	11.4	-0.8
	14.0	$12.8 \pm 1.4$	11.0	8.6
Standards				
20-HETE	0.75	$0.84 \pm 0.01$	1.7	-12.0
	1.0	$0.91 \pm 0.04$	4.3	8.8
	3.0	$2.9 \pm 0.2$	7.5	4.1
	6.0	$6.0 \pm 0.3$	4.3	0.3
	12.0	$12.0 \pm 0.1$	0.6	0.0
	16.0	$16.5 \pm 0.3$	2.0	-3.3

<sup>a</sup> A total of 12 quality control samples per concentration.

<sup>b</sup> Six to 12 quality control samples or two standards per day per concentration for 3 days.

Table 3  
Kinetic analysis of 20-HETE formation in rat brain, liver, and kidney microsomes

20-HETE	$V_{\max}$ (pmol/mg per min) (mean $\pm$ SE)	$K_m$ ( $\mu M$ ) (mean $\pm$ SE)
Brain	8.7 $\pm$ 0.6	39.9 $\pm$ 6.0
Liver	775.5 $\pm$ 39.8	23.5 $\pm$ 3.2
Kidney	1933 $\pm$ 151	47.6 $\pm$ 8.5

### 3.4. In vitro microsomal incubates

#### 3.4.1. Brain microsomes

In vitro 20-HETE formation in rat brain microsomes incubated with AA was evaluated. Formation of 20-HETE was linear up to 1000  $\mu g$  of total microsomal protein and over 80 min of incubation time (data not shown). In addition, formation of 20-HETE was determined to be saturable at an AA concentration of  $\sim 100 \mu M$  with a  $V_{\max}$  of  $8.7 \pm 0.6$  pmol/min per mg and a  $K_m$  of  $39.9 \pm 6.0 \mu M$  (Fig. 2A; Table 3).

#### 3.4.2. Liver and kidney microsomes

In vitro formation of 20-HETE in rat liver microsomes was determined to be saturable at an AA concentration of  $\sim 100 \mu M$  with a  $V_{\max}$  of  $775.5 \pm 39.8$  pmol/min per mg and a  $K_m$  of  $23.5 \pm 3.2 \mu M$  (Fig. 2B; Table 3). Likewise, in vitro 20-HETE formation in rat kidney microsomes was determined to be saturable at an AA concentration of  $\sim 100 \mu M$  with a  $V_{\max}$  of  $1933 \pm 151$  pmol/min per mg and a  $K_m$  of  $47.6 \pm 8.5 \mu M$  (Fig. 2C; Table 3).

## 4. Discussion

Recent studies have shown that 20-HETE is an important vasoactive mediator involved in the pathogenesis of various disease states in brain [2], liver [29], and kidney [30–32] tissue. Thus, sensitive and specific analytical methods for the detection and quantification of 20-HETE are needed to facilitate the further evaluation of the pathophysiologic role of 20-HETE. Although multiple, detailed methods for the determination of 20-HETE have been reported, published methods for the quantitation of 20-HETE

by HPLC–MS are lacking. Here we report a reproducible (% RSD < 15%) HPLC–MS method for quantification of 20-HETE in microsomal incubates that provides both sensitive (LOQ of 0.75 ng injected on column) and specific detection of 20-HETE in microsomal incubates. This method was used to determine the enzyme kinetics of 20-HETE formation in microsomal incubates from rat brain, liver, and kidney tissues.

The HPLC–MS method described circumvents difficulties associated with the conventional methods for determining 20-HETE, such as the use of radiolabeled AA substrate and/or derivatization of formed metabolites [20,21]. The HPLC–MS method utilizes non-radiolabeled substrate, which avoids the high cost of radiolabeled substrate and inconvenience of radioactive waste disposal. GC–MS [18,33,34] and fluorescence-HPLC [19] quantification involve analyte extraction and derivatization prior to analysis. The HPLC–MS method avoids derivatization allowing direct quantification of 20-HETE in samples following extraction.

Various solvents reported in the literature for the extraction of 20-HETE were systematically evaluated for extraction recovery of both 20-HETE and [ $^2H_8$ ]15(S)-HETE (Table 1). Diethyl ether, ethyl acetate, and dichloromethane extraction recoveries for 20-HETE and [ $^2H_8$ ]15(S)-HETE were similar and superior to hexane (Table 1). Acidification of samples with formic acid to final pH values less than 3.2 reduced the extraction recoveries of both 20-HETE and [ $^2H_8$ ]15(S)-HETE. Due to the decreased recoveries of metabolites in the presence of acid, microsomal incubates were not acidified prior to extraction and quantification.

The HPLC–MS method was used to determine the enzyme kinetics of 20-HETE formation in rat brain, liver, and kidney microsomal incubates. Formation of 20-HETE in each of the microsomal incubates was saturable at AA concentrations of  $\sim 100 \mu M$  (Fig. 2). The use of non-radiolabeled substrate provided a wider range of AA concentrations enabling saturable 20-HETE formation in microsomal incubates. Radiochemical-HPLC studies typically using 0.5–1  $\mu Ci$  of radiolabeled AA, yield non-saturating AA concentrations of  $\sim 10 \mu M$  [5,35]. Formation of 20-HETE should be evaluated at saturating substrate concentrations in order to ascertain changes in  $V_{\max}$  particularly when mechanisms



of CYP induction or overexpression are being evaluated. Additionally, saturating substrate concentrations represent physiologically relevant AA concentrations which have been reported as high as 300  $\mu\text{M}$  after cerebral ischemia [36,37].

The substrate saturation curves generated were used to determine enzyme kinetic parameters of 20-HETE formation in rat brain, liver, and kidney microsomal incubates. The enzyme kinetic data were best fit by a one-enzyme Michaelis-Menten model. Liver and kidney microsomal incubates yielded apparent  $V_{\text{max}}$  and  $K_{\text{m}}$  values (Fig. 2B,C; Table 3) that are consistent with reported formation rates (range 1–6 nmol/min per mg) and  $K_{\text{m}}$  values (20–40  $\mu\text{M}$ ) [38]. CYP4A1 and CYP4A3 isoforms are expressed constitutively in liver microsomes of male Sprague–Dawley rats [39].  $K_{\text{m}}$  values for 20-HETE formation in baculovirus-expressed CYP4A1 and CYP4A3 were reported to be 10 and 41  $\mu\text{M}$ , respectively [28]. In kidney microsomes of Sprague–Dawley rats high expression of CYP4A2 has been demonstrated [39]. The  $K_{\text{m}}$  value for 20-HETE formation in baculovirus-expressed CYP4A2 studies was determined to be 19  $\mu\text{M}$  [28]. Brain microsomal 20-HETE formation was linear with respect to time as well as protein concentration and saturable at  $\sim 100 \mu\text{M}$  AA (Fig. 1A). Enzyme kinetic parameters observed were a  $V_{\text{max}}$  of  $8.7 \pm 0.6$  pmol/min per mg and a  $K_{\text{m}}$  of  $39.9 \pm 6.0 \mu\text{M}$  (Table 3).

In conclusion, a reproducible, sensitive, and specific HPLC–MS method for quantification of 20-HETE in rat microsomal incubates was developed and validated. This method avoids difficulties associated with conventional methods for 20-HETE determination. The use of non-radiolabeled AA ensures in vitro 20-HETE formation to be determined at substrate concentrations that were saturating ( $V_{\text{max}}$ ) and physiologically relevant. The validated method was used for determining the enzyme kinetics of 20-HETE formation in brain, liver, and kidney microsomes. These studies report the first evaluation of the enzyme kinetics of CYP-dependent 20-HETE formation in the rat brain.

## Acknowledgements

This work was supported by a beginning grant-in-aid (02654424U) from the Pennsylvania-Delaware

affiliate of the American Heart Association, and a seed grant from the Pittsburgh Institute for Neurological Disorders (PIND). The technical assistance of Cheryl Galloway and Robert Reynolds is gratefully acknowledged. WinNonlin was provided by Pharsight Corporation (Mountainview, CA, USA) as part of their Pharsight Academic Learning Program.

## References

- [1] J.H. Capdevila, J.R. Falck, *Biochem. Biophys. Res. Commun.* 285 (2001) 571.
- [2] F. Kehl, L. Cambj-Sapunar, K.G. Maier, N. Miyata, S. Kametani, H. Okamoto, A.G. Hudetz, M.L. Schulte, D. Zagorac, D.R. Harder, R.J. Roman, *Am. J. Physiol. Heart Circ. Physiol.* 282 (2002) H1556.
- [3] J.H. Capdevila, J.R. Falck, R.C. Harris, *J. Lipid Res.* 41 (2000) 163.
- [4] W.L. Smith, D.L. DeWitt, R.M. Garavito, *Annu. Rev. Biochem.* 69 (2000) 145.
- [5] D.R. Harder, D. Gebremedhin, J. Narayanan, C. Jefcoat, J.R. Falck, W.B. Campbell, R.J. Roman, *Am. J. Physiol.* 266 (1994) H2098.
- [6] D. Gebremedhin, A.R. Lange, T.F. Lowry, M.R. Taheri, E.K. Birks, A.G. Hudetz, J. Narayanan, J.R. Falck, H. Okamoto, R.J. Roman, K. Nithipatikom, W.B. Campbell, D.R. Harder, *Circ. Res.* 87 (2000) 60.
- [7] J. Kaide, M.H. Wang, J.S. Wang, F. Zhang, V.R. Gopal, J.R. Falck, A. Nasjletti, M. Laniado-Schwartzman, *Am. J. Physiol. Renal Physiol.* 284 (2003) F51.
- [8] D.E. Stec, A. Flasch, R.J. Roman, J.A. White, *Am. J. Physiol. Renal Physiol.* 284 (2003) F95.
- [9] J.D. Imig, A.P. Zou, D.E. Stec, D.R. Harder, J.R. Falck, R.J. Roman, *Am. J. Physiol.* 270 (1996) R217.
- [10] M.H. Wang, H. Guan, X. Nguyen, B.A. Zand, A. Nasjletti, M.L. Schwartzman, *Am. J. Physiol.* 276 (1999) F246.
- [11] R.J. Roman, *Physiol. Rev.* 82 (2002) 131.
- [12] M. Alonso-Galicia, K.G. Maier, A.S. Greene, A.W. Cowley Jr., R.J. Roman, *Am. J. Physiol. Regul. Integr. Comp. Physiol.* 283 (2002) R60.
- [13] H.C. Hercule, A.O. Oyekan, *J. Pharmacol. Exp. Ther.* 292 (2000) 1153.
- [14] M. Alonso-Galicia, C.W. Sun, J.R. Falck, D.R. Harder, R.J. Roman, *Am. J. Physiol.* 275 (1998) F370.
- [15] C.W. Sun, J.R. Falck, H. Okamoto, D.R. Harder, R.J. Roman, *Am. J. Physiol. Heart Circ. Physiol.* 279 (2000) H339.
- [16] X. Hou, F. Gobeil Jr., K. Peri, G. Speranza, A.M. Marrache, P. Lachapelle, J. Roberts, D.R. Varma, S. Chemtob, E.F. Ellis, *Stroke* 31 (2000) 516.
- [17] A.P. Zou, J.T. Fleming, J.R. Falck, E.R. Jacobs, D. Gebremedhin, D.R. Harder, R.J. Roman, *Am. J. Physiol.* 270 (1996) R228.
- [18] M. Zemaitis, S. Poloyac, R. Frye, *Rapid Commun. Mass Spectrom.* 16 (2002) 1411.

- [19] K.G. Maier, L. Henderson, J. Narayanan, M. Alonso-Galicia, J.R. Falck, R.J. Roman, *Am. J. Physiol. Heart Circ. Physiol.* 279 (2000) H863.
- [20] M.C. Romano, K.E. Straub, L.P. Yodis, R.D. Eckardt, J.F. Newton, *Anal. Biochem.* 170 (1988) 83.
- [21] G. Luo, D.C. Zeldin, J.A. Blaisdell, E. Hodgson, J.A. Goldstein, *Arch. Biochem. Biophys.* 357 (1998) 45.
- [22] J. Bylund, J. Ericsson, E.H. Oliw, *Anal. Biochem.* 265 (1998) 55.
- [23] K. Nithipatikom, A.J. Grall, B.B. Holmes, D.R. Harder, J.R. Falck, W.B. Campbell, *Anal. Biochem.* 298 (2001) 327.
- [24] J.W. Newman, T. Watanabe, B.D. Hammock, *J. Lipid Res.* 43 (2002) 1563.
- [25] N. Tindberg, H.A. Baldwin, A.J. Cross, M. Ingelman-Sundberg, *Mol. Pharmacol.* 50 (1996) 1065.
- [26] O.H. Lowry, N.J. Rosebrough, A.L. Farr, R.J. Randall, *J. Biol. Chem.* 193 (1951) 265.
- [27] T. Omura, R. Sato, *J. Biol. Chem.* 239 (1964) 2379.
- [28] X. Nguyen, M.H. Wang, K.M. Reddy, J.R. Falck, M.L. Schwartzman, *Am. J. Physiol.* 276 (1999) R1691.
- [29] D. Sacerdoti, M. Balazy, P. Angeli, A. Gatta, *J. Clin. Invest.* 100 (1997) 1264.
- [30] M.H. Wang, H. Guan, X. Nguyen, B.A. Zand, A. Nasjletti, M. Laniado-Schwartzman, *Am. J. Physiol.* 276 (1999) F246.
- [31] M.H. Wang, F. Zhang, J. Marji, B.A. Zand, A. Nasjletti, M. Laniado-Schwartzman, *Am. J. Physiol. Regul. Integr. Comp. Physiol.* 280 (2001) R255.
- [32] D.L. Kroetz, L.M. Huse, A. Thuresson, M.P. Grillo, *Mol. Pharmacol.* 52 (1997) 362.
- [33] B. Watzet, S. Reinalter, H.W. Seyberth, H. Schweer, *Prostaglandins Leukot. Essent. Fatty Acids* 62 (2000) 175.
- [34] K. Nithipatikom, R.F. DiCamelli, S. Kohler, R.J. Gumina, J.R. Falck, W.B. Campbell, G.J. Gross, *Anal. Biochem.* 292 (2001) 115.
- [35] Y. Amet, A. Zerilli, T. Goasduff, Y. Dreano, F. Berthou, *Biochem. Pharmacol.* 54 (1997) 947.
- [36] P. Lipton, *Physiol. Rev.* 79 (1999) 1431.
- [37] N.G. Bazan, *Adv. Exp. Med. Biol.* 72 (1976) 317.
- [38] J.H. Capdevila, R.C. Harris, J.R. Falck, *Cell Mol. Life Sci.* 59 (2002) 780.
- [39] J.R. Okita, S.B. Johnson, P.J. Castle, S.C. Dezelle, R.T. Okita, *Drug Metab. Dispos.* 25 (1997) 1008.